Journal of Nuclear Materials 415 (2011) S701–S704

Contents lists available at ScienceDirect

Journal of Nuclear Materials

journal homepage: www.elsevier.com/locate/jnucmat

Dynamics of hydrogen isotope trapping and detrapping for tungsten under simultaneous triple ion (C^+, D_2^+ and He^+) implantation

Yasuhisa Oya [a,*,1], Makoto Kobayashi [a], Rie Kurata [a], Wanjing Wang [a], Naoko Ashikawa [b], Akio Sagara [b], Naoaki Yoshida [c], Yuji Hatano [d], Kenji Okuno [a]

[a] Radioscience Research Laboratory, Faculty of Science, Shizuoka University, 836, Ohya, Suruga-ku, Shizuoka 422-8529, Japan
[b] National Institute for Fusion Science, 322-6 Oroshi-cho, Toki-shi, Gifu 509-5292, Japan
[c] Institute for Applied Mechanics, Kyushu University, Kasuga, Fukuoka 816-8580, Japan
[d] Hydrogen Isotope Research Center, University of Toyama, 3190, Gofuku, Toyama 930-8555, Japan

ARTICLE INFO

Article history:
Available online 3 November 2010

ABSTRACT

To elucidate the simultaneous implantation effects on deuterium retention in polycrystalline tungsten, simultaneous 10 keV C^+, 3 keV D_2^+ and 3 keV He^+ implantation was performed at room temperature. He^+/D^+ flux ratio dependence of deuterium retention indicated that He^+ implantation induced high deuterium retention even if the He^+/D^+ flux ratio was low. D_2 TDS spectrum for C^+–D_2^+ implanted tungsten was clearly different from the samples with only D_2^+, D_2^+–He^+ and C^+–D_2^+–He^+ implantation, indicating that D was trapped by C as C–D bond. For D_2^+–He^+ implantation sample, He^+ implantation would introduce irradiation damages and D retention increased. However, C^+–D_2^+–He^+ implantation, the accumulation of C on tungsten was suppressed and the retention of D trapped by C clearly decreased. These facts indicated the D retention for C^+–D_2^+–He^+ implanted tungsten was limited by He^+ implantation and most of D would be retained in the interstitial sites or irradiation defects under simultaneous implantation with He.

1. Introduction

Retention of hydrogen isotope including tritium in plasma facing materials is one of key issues for the fuel management [1,2]. Recently, tungsten was considered one of the candidates for plasma facing materials especially for the divertor armor except for the strike points where CFC will be used [3–7]. Therefore, it is anticipated that the some carbon will be sputtered by high heat flux and the carbon ions will be formed and transported to tungsten surface with energetic hydrogen isotopes including tritium from plasma, which would enhance high tritium retention on tungsten surface. In addition, many researchers reported that implantation of helium, which will be produced by fusion reaction, also could induce high tritium retention [8] and surface modification [9]. Helium bubbles were formed and surface structure was clearly reconstructed, which would also lead to the high tritium retention. Therefore, it is quite important to evaluate the hydrogen isotope retention under the simultaneous C^+, D_2^+ and He^+ implantation environment.

In our previous studies [10–12], the simultaneous C^+ and D_2^+ implantation was performed on tungsten and the D retention was evaluated as a function of C^+/D^+ flux ratio. It was found that at low C^+/D^+ flux ratio, D retention was large, indicating that the C^+/D^+ flux ratio plays one of key roles for the deuterium trapping. It was also reported that the formation of C–C layer would enhance the chemical sputtering of carbon by deuterium and the chemical state of carbon would control the deuterium retention on tungsten under C^+–D_2^+ implantation. It was also reported that D retention was decreased when He^+ was added to the incident beam, namely triple ion (C^+–D_2^+–He^+) implantation. These results indicate that He implantation would make large contribution not only to D retention but also to C retention/accumulation. Therefore, in the present study, simultaneous implantation of He^+–D_2^+ was performed at the different He^+/D^+ flux ratio and He implantation effect on D retention was studied. In addition, microstructure change by triple or dual ion implantation was compared and triple implantation effect on D retention was discussed.

2. Experimental

The disk-type samples with 10 mm diameter and 0.5 mm thickness were prepared from a rod of tungsten under stress-relieved conditions (heated at 1173 K) supplied by Allied Tungsten Co. Ltd. The samples were polished mechanically by SiC carbimet paper and diamond suspensions, and thereafter pre-heated at 1173 K for 10 min in vacuum to remove the surface impurities and damage induced by the polishing process.

* Corresponding author. Tel.: +81 54 238 4803; fax: +81 54 238 3989.
E-mail address: syoya@ipc.shizuoka.ac.jp (Y. Oya).
1 Presenting author.

0022-3115/$ - see front matter © 2010 Elsevier B.V. All rights reserved.
doi:10.1016/j.jnucmat.2010.09.058

The simultaneous carbon ion (C^+), deuterium ion (D_2^+) and helium ion (He^+) implantation system combined with a TDS (thermal desorption spectroscopy) system was designed and established at Shizuoka University. The sample can be easily transferred from the ion implantation chamber to the TDS chamber via a sample introduction chamber without air exposure. The C^+, D_2^+ and He^+ were implanted using different ion guns equipped in the implantation chamber. The implantation angle for C^+ was 0° with respect to the surface normal and that for D_2^+ and He^+ was 30°. CO_2 was used as C^+ source gas to exclude hydrogen impurities. The $E \times B$ mass separator was equipped at the head of the C^+ gun and the oxygen impurity was completely evacuated by a turbo molecular pump. The implantation area was set to be 4 mm × 4 mm. C^+ acceleration energy was controlled to be 10 keV and the ion flux was estimated by a faraday cup. A ceramic heater was equipped with the sample holder to heat up to 1300 K.

In the present study, to elucidate the influence of C and He on D retention in tungsten, it is important to keep the mean implantation depth of C^+ and He^+ same as that of D_2^+. SRIM calculation shows that the mean implantation depth of 3 keV D_2^+ and He^+ is almost the same as that of 10 keV C^+; corresponding to the mean implantation depth of ~11 nm [13]. Therefore, the ion energies of C^+, D_2^+ and He^+ were set to be 10 keV, 3 keV and 3 keV respectively.

D_2^+–He^+ implantation experiments were performed to evaluate He mixing effect on D retention as a function of He^+/D^+ flux ratio of 0.2, 1.0 and 1.8 at room temperature. D flux was set to be 1.0×10^{18} D^+ m^{-2} s^{-1} up to a fluence of 1.0×10^{22} D^+ m^{-2}. He flux was changed from 0.2×10^{18} He^+ m^{-2} s^{-1} to 1.8×10^{18} He^+ m^{-2} s^{-1}. After the ion implantation experiment, TDS measurement was carried out at a heating rate of 0.5 K s^{-1} up to 1300 K, desorbed particles were detected by a high resolution quadrupole mass spectrometer, which can separate D_2 and He. TEM (transmission electron microscopy) observations (JEM 2000EX, JASCO Inc.) were performed at the Institute of Applied Mechanics, Kyushu University to analyze the microstructure of the triple and dual ions implanted tungsten. D depth profile was evaluated by GD-OES (Glow Discharge Optical Emission Spectroscopy, GD-Profiler 2, Horiba Inc.) at University of Toyama.

For the comparison of C^+–D_2^+ and D_2^+–He^+ dual implantation with C^+–D_2^+–He^+ triple implantation, the fluxes of C^+, D_2^+ and He^+ were set to be 0.2×10^{18} C^+ m^{-2} s^{-1}, 1.0×10^{18} D^+ m^{-2} s^{-1} and 0.2×10^{18} He^+ m^{-2} s^{-1} to keep the flux ratio of C^+:D^+:He^+ = 0.2:1.0:0.2 and simultaneous implantations with various combination of C^+, D^+ and He^+ were performed up to the D fluence of 1.0×10^{22} D^+ m^{-2}. All the ion implantation experiments were done at room temperature. Thereafter, TDS measurement and TEM observation were also performed. Before and after ions implantation, XPS (X-ray photoelectron spectroscopy) (ESCA1600 system, ULVAC-PHI Inc.) measurements were also carried out to evaluate the chemical state of C on tungsten surface.

3. Results and discussion

Fig. 1a shows D_2 TDS spectra for the D_2^+–He^+ implanted tungsten as a function of He^+/D^+ flux ratio. The D_2 TDS spectrum for only D_2 implanted tungsten is also shown. It was found that D_2 desorption takes place in the temperature region of 400–700 K with the maximum at 450 K. Irradiation by He^+ and D_2^+ mixed ion beam with different ion flux ratio showed no change on the spectra shape, indicating no impact of He^+/D^+ flux ratio on the D_2 desorption. In Fig. 1b, D depth profiles within the depth of 50 nm are showed by GE-OES measurement. These results indicated that D distribution in tungsten was almost the same for all He^+/D^+ flux ratios, which is consistent with TDS results. Most of D was retained

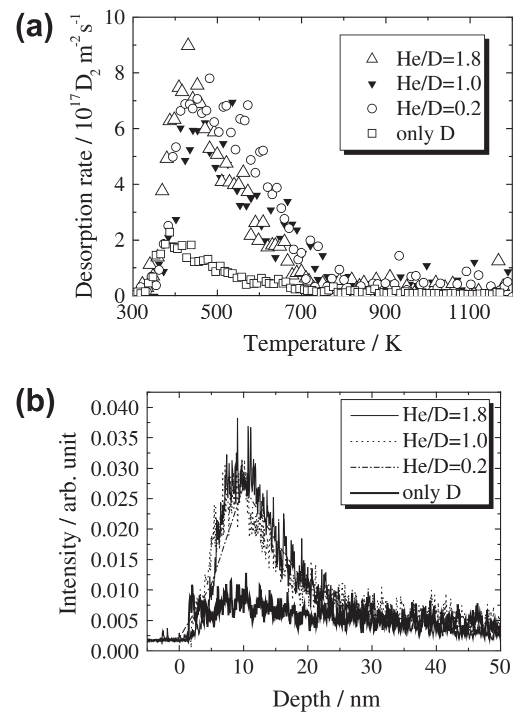

Fig. 1. D_2 TDS spectra (a) and D depth profiles (b) for simultaneously He^+–D_2^+ implanted tungsten as a function of He^+/D^+ flux ratio.

within the depth of 20 nm with the maximum at 10 nm, which is consistent with the SRIM estimation. D depth profiles for D_2^+–He^+ implanted tungsten are clearly different from that for only D_2 implanted one. Fig. 2 summarizes D retention as a function of He^+/D^+ flux ratio. It was shown that D retention is almost constant by changing the He^+/D^+ flux ratio and it was about five times as high as that for only D_2^+ implantation. In the previous paper, S. Nagata reported that D retention was strongly enhanced by He pre-irradiation up to a small dose where a large distortion was creased at room temperature [8]. This fact indicates that the irradiation defects induce the D accumulation at the implantation depth. On the other hand, He bubbles would prevent D diffusion toward the depth like diffusion barrier, because no D accumulation was observed for only D_2^+ implantation as shown in GD-OES results. In addition, D retention was almost constant in He^+ fluence between 10^{19} and 10^{21} m^{-2}. TEM micrographs for the simultaneous D_2^+–He^+ implanted tungsten with the He^+/D^+ flux ratio of 0.2, 1.0 and 1.8 are summarized in Fig. 3. Two pictures for each specimen are shown; one is the micrograph just after the implantation

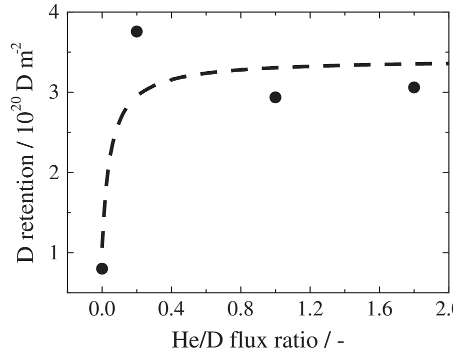

Fig. 2. D retention for simultaneous He^+–D_2^+ implanted tungsten as a function of He^+/D^+ flux ratio.

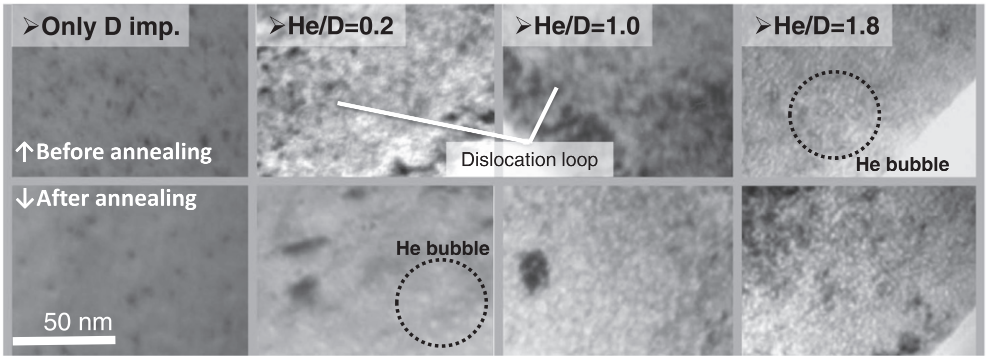

Fig. 3. TEM micrographs for the simultaneously He^+–D_2^+ implanted tungsten with the He^+/D^+ flux ratio of 0.2, 1.0 and 1.8. Two pictures for each specimen are shown. One is the micrograph just after the implantation (before annealing), and the other is that after heating at 1073 K (after annealing).

(Before annealing), and the other is after heating at 1073 K (After annealing). Before the implantation, no major defects were observed. The dislocations and dislocation loops were observed for the samples with low He^+/D^+ flux ratios of 0.2 and 1.0 before annealing. However, He bubbles were only observed for the sample with He^+/D^+ flux ratio of 1.8. After annealing at 1073 K, He bubbles were observed for all the samples, indicating that He was retained in all samples and it was accumulated by annealing. The density of He bubbles for the sample with He^+/D^+ flux ratio of 1.8 was the highest, which reflects large He retention.

D_2 TDS spectra for various simultaneous ion implantation conditions are compared in Fig. 4. It was found that D_2 desorption for the only D_2^+ implanted tungsten takes place at low temperature of less than 600 K. The shape of D_2 TDS spectrum for the C^+–D_2^+ implanted tungsten is quite different from the other spectra. The large amount of deuterium desorbed at higher temperature of 800–1000 K and the spectra consisted of three stages, as one can see from Fig. 4. For D_2^+–He^+ implanted tungsten, D_2 desorption stage is concentrated on the lower temperature side less than 700 K. For the triple ion beam (C^+, D_2^+ and He^+) implantation, the desorption temperature is almost the same as that for only D_2^+ implanted tungsten and D_2^+–He^+ implanted tungsten. Mixing of C^+ and/or He^+ with D_2^+ resulted in increase of D retention about three times as that for the only D_2^+ implanted tungsten. By the triple ion beam implantation, D retention was reduced as compared to C^+–D_2^+ and He^+–D_2^+ cases. Similar to He^+–D_2^+ case, TDS spectrum for C^+–He^+–D_2^+ case is clearly different from that for C^+–D_2^+ implanted tungsten as mentioned above. This indicates that C^+ implantation would enhance the sputtering as mentioned in Ref. [12] and He^+ implantation also introduce the irradiation damages. To evaluate the microstructure change by C^+–D_2^+ implantation and

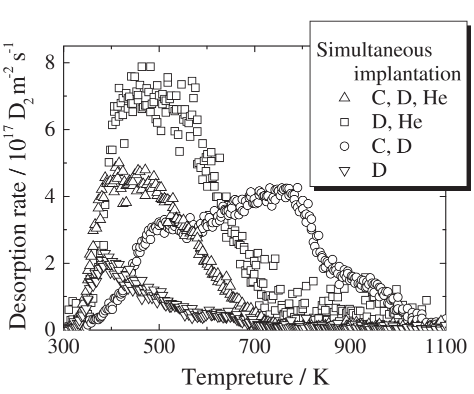

Fig. 4. D_2 TDS spectra for only D_2^+ and for simultaneously C^+–D_2^+, D_2^+–He^+ and C^+–D_2^+–He^+ implanted samples.

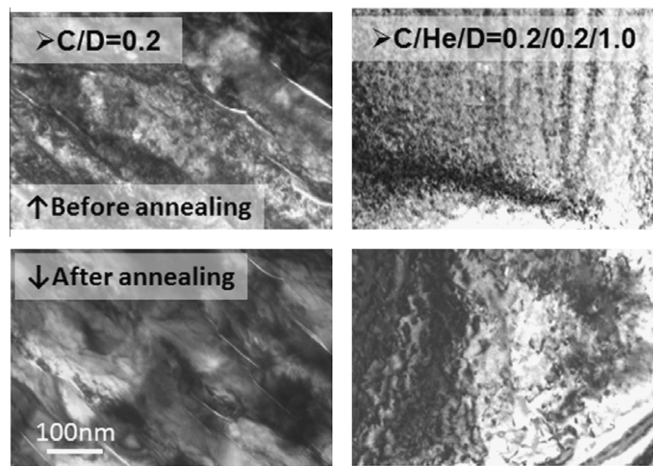

Fig. 5. TEM micrographs for simultaneously C^+–D_2^+ and C^+–D_2^+–He^+ implanted samples.

C^+–D_2^+–He^+ implantation, TEM micrographs are shown in Fig. 5. It was found that large amount of micro irradiation defects were introduced by the C^+–D_2^+ implantation and dislocation loops did not annealed after the heating at 1073 K. In the case of C^+–D_2^+–He^+ implantation, the high density of dislocation loops around a few nanometer was produced by the ion implantation, indicating that C^+ and He^+ implantation introduces irradiation damages in addition to D sputtering.

To evaluate the interaction with carbon which was implanted into tungsten, XPS measurements were performed. In Fig. 6, C-1s XPS spectra for only C^+, C^+–D_2^+ and C^+–D_2^+–He^+ implanted tungsten samples showed that the C–C concentration for C^+–D_2^+–He^+ implanted tungsten was lower than that for C^+–D_2^+ implanted tungsten, indicating the He^+ implantation prevent the C accumulation, especially the formation of C–C bond, on tungsten. Therefore, the major chemical state of C on tungsten surface would be the C–W bond and the C concentration was clearly low compared to that for C^+–D_2^+ implanted tungsten. These facts indicate that trapping of D by C was quite limited for C^+–D_2^+–He^+ implanted tungsten and no D desorption was observed at higher temperature of 800 K.

From these experimental results, simultaneous implantation effect on deuterium trapping in tungsten is discussed. D retention was clearly changed by combination of ion sources. Large D retention was found for C^+–D_2^+ and D_2^+–He^+ implanted tungsten. However, the desorption stages among these samples were clearly different and large desorption stage for C^+–D_2^+ implanted sample was found at higher temperature region of 800 K, although D desorption for D_2^+–He^+ implanted tungsten was concentrated on

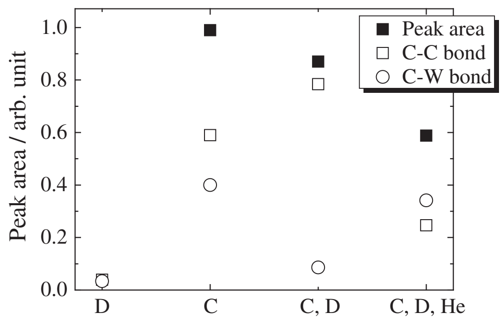

Fig. 6. Peak areas and, C–C, C–W chemical states for C-1s XPS spectra for D_2^+, C^+, C^+–D_2^+ and C^+–D_2^+–He^+ implanted samples.

lower temperature less than 700 K indicating that major deuterium trapping for C^+–D_2^+ case should be C–D bond. For D_2^+–He^+ implantation, He retention would introduce additional irradiation defects and prevent D diffusion toward the depth and/or D desorption, which lead the. D accumulation beneath the surface. Therefore, D retention was limited and most of D would be retained in the interstitial sites and/or irradiation defects, showing the D desorption was proceeded at lower temperature region. For the C^+–D_2^+–He^+ implanted case, C^+ and He^+ were retained during the implantation process. However, He^+ implantation also induces the removal of carbon layer and interferes the D and C accumulation. Some residual carbon would be bound to tungsten with forming C–W bond. The retained He would also prevent D trapping and diffusion toward the depth and D retention would be suppressed. In the present study, the implantation depth for all ion sources was set to be the same and the contribution between D trapping by C and D accumulation by He diffusion barrier was still not clear. In the further study, the ion energies for C^+ and He^+ will be changed and D retention behavior will be studied as a function of implantation depth.

4. Conclusion

Simultaneous C^+, D_2^+ and He^+ implantation was performed to elucidate the effects on D retention in tungsten, D retention was compared with C^+–D_2^+ and D_2^+–He^+ implantation cases. In addition, He^+/D^+ flux ratio dependence on deuterium retention was also evaluated. It was found that He implantation induced high deuterium retention even if the He^+/D^+ flux ratio was low, compared to only D_2^+ case. D_2 TDS spectrum for C^+–D_2^+ implanted tungsten was clearly different from the other samples and D_2 desorption stage was extended to higher temperature side above 800 K. For D_2^+–He^+ and C^+–D_2^+–He^+ implanted samples, D_2 desorption stage was concentrated on lower temperature side less than 700 K. Large amount of D desorption at temperature between 400 and 700 K was found for D_2^+–He^+ implanted sample, indicating that He^+ irradiation would introduce the irradiation defects and its retention would prevent the D diffusion toward the depth and/or D desorption. In the case of C^+–D_2^+ implantation, the C was accumulated on tungsten and D was trapped by C as C–D bond. However, C accumulation was suppressed for C^+–D_2^+–He^+ case, which led to the reduction of D retention. These facts indicated the D retention for C^+–D_2^+–He^+ implanted tungsten was limited by He^+ implantation and most of D would be retained in the interstitial sites or irradiation defects under simultaneous implantation with He.

Acknowledgements

This study has been supported by NIFS Collaboration Program No. NIFS07KOBA020, JSPS Kakenhi Nos. 19686055 and 22360389 from MEXT, Japan, and the Center for Instrumental Analysis at Shizuoka University.

References

[1] J. Roth, E. Tsitrone, A. Loarte, et al., J. Nucl. Mater. 390–391 (2009) 1–9.
[2] T. Loarer, J. Nucl. Mater. 390–391 (2009) 20–28.
[3] Y. Ueda, M. Fukumoto, A. Yamawaki, et al., J. Nucl. Mater. 390–391 (2009) 44–48.
[4] M. Kaufmann, R. Neu, Fusion Eng. Des. 82 (2007) 521–527.
[5] J. Pamela, G.F. Matthews, V. Philipps, R. Kamendje, JET-EFDA Contributors, J. Nucl. Mater. 363–365 (2007) 1–11.
[6] R.P. Doerner, J. Nucl. Mater. 363–365 (2007) 32–40.
[7] I. Bizyukov, K. Krieger, N. Azarenkov, Ch. Linsmeier, S. Levchuk, J. Nucl. Mater. 363–365 (2007) 1184–1189.
[8] S. Nagata, K. Takahiro, J. Nucl. Mater. 290–293 (2001) 135–139.
[9] M.J. Baldwin, R.P. Doerner, D. Nishijima, et al., J. Nucl. Mater. 390–391 (2009) 886–890.
[10] Y. Oya, Y. Inagaki, S. Suzuki, et al., J. Nucl. Mater. 390–391 (2009) 622–625.
[11] Y. Oya, S. Suzuki, W. Wang, et al., Phys. Scr. T138 (2009) 014051.
[12] M. Kobayashi, S. Suzuki, W. Wang, et al., Phys. Scr. T138 (2009) 014050.
[13] J.F. Ziegler, SRIM code. 2006. <http://www.srim.org/>.